Mitochondrial targeting sequence of the influenza A virus PB1-F2 protein and its function in mitochondria

Hiroshi Yamada, Ritsu Chounan, Youichirou Higashi, Naoki Kurihara, Hiroshi Kido*

Division of Enzyme Chemistry, Institute for Enzyme Research, The University of Tokushima, Kuramoto-cho 3-18-15, 770-8503, Japan

Received 3 August 2004; revised 26 October 2004; accepted 9 November 2004

Available online 20 November 2004

Edited by Hans-Dieter Klenk

Abstract The influenza A virus PB1-F2 protein predominantly localizes in the mitochondria of virus-infected cells. A series of cDNAs encoding N- and C-terminal deletion mutants and site-directed mutagenesis of the basic residues of PB1-F2 appended to 3xFLAG revealed the domain from residues 46 to 75 to be both necessary and sufficient for mitochondrial targeting. In addition, the subdomain residues 63–75 and both Lys73 and Arg75 are minimally required for mitochondrial localization. Transfection of untagged- and 3xFLAG tagged-PB1-F2 into Vero, HeLa and MDCK cells changed the mitochondrial morphology from a filamentous to a dotted structure and suppressed the inner-membrane potential.

Keywords: PB1-F2 protein; Influenza A virus; Mitochondrion; Targeting sequence; Mitochondrial membrane potential

1. Introduction

Influenza A virus (IAV) is one of the most common infectious pathogens in both humans and animals, and causes considerable morbidity and mortality [1]. The pathogenicity of IAV is complex, being influenced by each of the eight RNA gene segments that are known to encode the viral 10 proteins with an additional small protein recently found and termed PB1-F2, the open reading frame of which overlaps the PB1 open reading frame [2,3]. Viral RNA replication is carried out through the concerted action of three polymerase subunits (PA, PB1 and PB2) and nucleoprotein and the resulting nucleocapsids are exported from the nucleus via the proteins M1 and NS2 [4–10].

Besides the role of these viral proteins in viral proliferation, it has been reported that many viral factors induce cell injury and apoptosis of the infected cells. Viral proteins PB2 and M inhibit mitochondrial β-oxidation [11,12] and PB1-F2 predominantly suppresses the mitochondrial inner-membrane potential [2,3]. In the process of influenza virus replication, virus generates double-stranded RNA (dsRNA) and dsRNA-activated protein kinase (PKR). The activated PKR induces both Fas and Fas-ligand, which in turn induce caspases, a family of cysteine proteases structurally related to interleukin-1-β-converting enzyme, which are related to apoptosis [13–16]. In addition, other viral proteins, such as neuraminidase and hemagglutinin, induce apoptosis by direct activation of latent transforming growth factor-β [17] or alteration of the intracellular redox conditions [18]. Conflicting results of influenza virus NS1 protein as an inducer of apoptosis [19] and an anti-apoptotic regulator [20] have been reported.

In the present study, we analyzed the molecular mechanisms of mitochondrial targeting and the functions of a new member of the influenza virus proteins, PB1-F2. To analyze intracellular localization of PB1-F2, we initially made a chimeric protein consisting of 10.5 kDa of PB1-F2 genetically fused to 29 kDa of enhanced green fluorescent protein (EGFP) as reported [3]. However, we were able to detect only a small percentage (less than 15–20%) of mitochondrial localization of chimeric PB1-F2 in the PB1-F2-positive HeLa and Vero cells, and most of the chimeric protein was found in the cytosol, with the percentage value of mitochondrial localization being significantly lower than that in MDBK cells infected with the influenza virus PR8 [3]. The difference may be due to a steric hindrance of the chimeric PB1-F2 protein by linkage with the relatively large acidic reporter protein EGFP. We made a chimeric PB1-F2 fused to a small reporter protein, 3xFLAG, with a molecular mass of 2.9 kDa instead of the large EGFP. Under these conditions, we found that most of the chimeric protein efficiently (about 70–80%) localizes in mitochondria and the predicted mitochondrial targeting sequence (MTS) was different from those previously reported by analysis of the chimeric PB1-F2-EGFP [3], although the C-terminal region of the newly identified MTS overlaps the N-terminal region of the reported MTS. We report here the PB1-F2 domain necessary and sufficient for mitochondrial localization, and also demonstrate that full-length PB1-F2 as well as deletion mutants localizing in mitochondria show a loss of mitochondrial potential and mitochondrial rounding.

2. Materials and methods

2.1. Cells and a virus

Vero and MDCK cells in Eagle's minimum essential medium and HeLa cells in Dulbecco's minimum essential medium, supplemented with 10% fetal calf serum, were grown as monolayers. Influenza virus A/Puerto Rico/8/34 (H1N1) (PR8) (Mt. Sinai strain) was used in this study. The virus was propagated and titrated in MDCK cells. Vero, HeLa and MDCK cells were infected at a m.o.i. of 5 plaque forming units per cell.

2.2. Construction of expression plasmids

The PB1-F2 coding sequence was amplified by PCR from the plasmid pBMSA-PB1 coding influenza A virus PR8 PB1 (purchased from Riken). PB1-F2 was cloned in the pEGFP-N1 expressing vector (Clontech) using the upstream (5′) primer CTTCTCGAGATGG-

*Corresponding author. Fax: +81 88 633 7425.
E-mail address: kido@ier.tokushima-u.ac.jp (H. Kido).

0014-5793/$22.00
doi:10.1016/j.febslet.2004.11.017

GACAGGAACAGGATACAC containing an initiation codon and *Xho*I site, and the downstream (3′) primer AGCGAATTCAC-TCGTGTTTGCTGAACAACCT containing a stop codon and *Eco*RI site. For cloning of PB1-F2 with 3xFLAG tag in the p3xFLAG-myc-CMV-26 expressing vector (Sigma), we used the 5′ primer containing an initiation codon and *Hind*III site, and the 3′ primer containing a stop codon and *Eco*RI site. For cloning of PB1-F2 with EGFP in the pEGFP-C3 expressing vectors (Clontech), we used the 5′ primer containing an initiation codon and *Xho*I site, and the 3′ primer containing a stop codon and *Eco*RI site. The nomenclature of the N- and C-terminal deletion mutants indicates the deleted amino acids; for example, 3xFLAG-31/75 indicates a truncated PB1-F2 protein containing amino acids 31–75 N-terminally fused to the 3xFLAG tag. All N- and C-terminal deletion mutants were made by using 5′ primers containing introduced initiation codons and by using 3′ primers containing introduced termination codons, respectively. The point mutants were made by substituting Lys and Arg residues with Ala. The nomenclature of the point mutants indicates the substituted amino acids; for example, 3xFLAG-K73A/R75A indicates a mutated PB1-F2 protein containing a Lys73-to-Ala and an Arg75-to-Ala mutation. All point mutants were made by using the 3′ primers with the desired mutations; for example, 3xFLAG-K73A/R75A was made with the 3′ primer GTCGAATTCTACTCGTGTTTGCTGAACAACCTCCA-TCGTTTCAATACAGCAGTTGCCAAAAATAC. The correctness of the plasmid constructs was analyzed by DNA sequencing. The expression of the size of plasmid constructs was confirmed by Western blotting.

2.3. Preparation of PB1-F2 antibodies

For cloning of PB1-F2 in the *Escherichia coli* (*E. coli*) expression vector pET-21a (Novagen), we used the 5′ primer containing an initiation codon and *Eco*RI site, and the 3′ primer containing *Xho*I site without a stop codon. PB1-F2-6xHis fusion protein was purified using HiTrap Chelating HP (Amersham BioSciences). Purified 1 mg PB1-F2-6xHis fusion protein in 1 ml saline was emulsified with an equal volume of complete Freund's adjuvant for the primary injection and with the incomplete form for booster injection, and injected into a Japan white rabbit several times at 3-week intervals. Antiserum with a satisfactory titer was applied to an affinity column of immunogen-coupled epoxy-activated Sepharose 6B and antigen-specific antibodies were obtained by elution with 0.2 M glycine/HCl buffer, pH 2.8.

2.4. Transfection and immunofluorescence detection

Vero, HeLa and MDCK cells were transfected by using FuGENE 6 transfection reagent (Roche) according to the manufacturer's instructions. The indirect immunofluorescence assay was performed as described previously [21,22]. Mouse monoclonal and rabbit polyclonal antibodies against the FLAG tag (Sigma) and rabbit polyclonal antibodies against PB1-F2 were used for immunofluorescence detection. Mouse monoclonal antibodies against the native form of cytochrome *c* were purchased from PharMingen. Rabbit anti-influenza A, B antibodies were purchased from Takara. Annexin V with Alexa Fluor 594 conjugate (Molecular Probes) was used according to the manufacturer's instructions. Mitochondrial transmembrane potential was monitored using MitoTracker Red CMXRos (Molecular Probes), tetramethylrhodamine ethyl ester (TMRE) (Molecular Probes) and Rhodamine 123 (Molecular Probes). pDSRed2-Mito was from Clontech. Fluorescent images were viewed and recorded with Zeiss Axioplan 2 microscopes. For each plasmid construction, over 500 PB1-F2-expressing cells in at least 15 randomly selected high power fields (400×) were counted to calculate percentage of the cells with PB1-F2 within mitochondria.

3. Results

3.1. Efficient mitochondrial targeting of 3xFLAG-PB1-F2

The subcellular localization of PB1-F2 in Vero cells at 24 h after transfection was analyzed by immunofluorescence assay. PB1-F2 localization in the mitochondria was found in 73 ± 4% of the PB1-F2-positive cells, as identified by the colocalization with MitoTracker Red dye (Fig. 1A–C). In the rest of the PB1-F2-positive cells, it was distributed in the cytoplasm and nucleus (data not shown). Subcellular localization of PB1-F2 with 3xFLAG tag in mitochondria was also found in

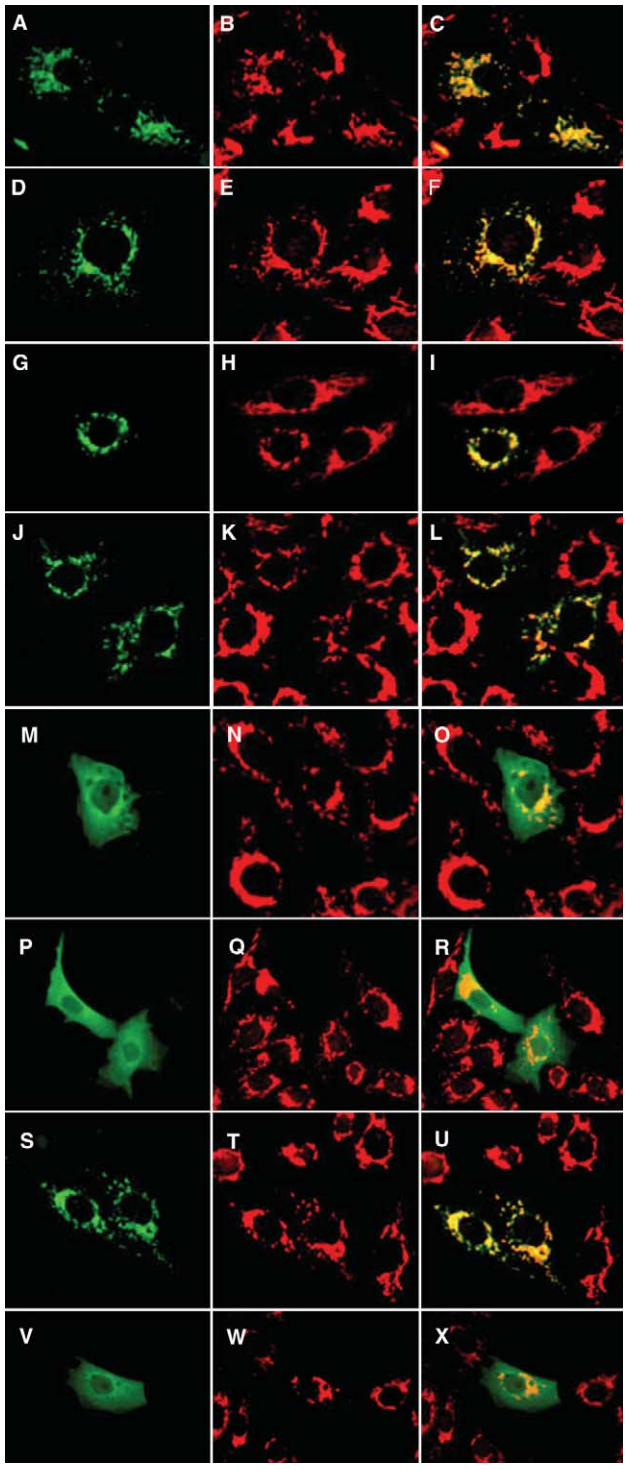

Fig. 1. Intracellular localization of untagged and tagged PB1-F2 fusion constructs. Vero cells transfected with plasmids expressing PB1-F2 (A–C), 3xFLAG-PB1-F2-1/87 (D–F), EGFP-PB1-F2-1/87 (G–I), 3xFLAG-46/75 (J–L), 3xFLAG-63/75 (M–O), EGFP-PB1-F2-63/75 (P–R), 3xFLAG-PB1-F2-78K/79R/81R (S–U) and 3xFLAG-PB1-F2-73K/75R (V–X) were incubated with MitoTracker Red and were fixed 24 h after transfection and labeled with mouse anti-FLAG monoclonal antibodies and FITC-conjugated anti-mouse antibodies.

75 ± 4% of 3xFLAG-PB1-F2-positive cells, but the localization of PB1-F2 with EGFP was found only in 14 ± 1.5% of EGFP-PB1-F2-positive cells (Fig. 1G–I). In addition, as reported also for PR8-infected cells, certain cells expressing mitochondrial 3xFLAG-PB1-F2 exhibited a loss of mitochondrial membrane potential, as indicated by decreased staining with MitoTracker Red and alteration of the mitochondrial morphology from tubular to rounded and vesicular forms (Fig. 3A–I) [2,3]. These results suggest that a chimeric PB1-F2 fused to a small 3xFLAG instead of the large acidic EGFP well reflects the subcellular localization of native PB1-F2.

3.2. The mitochondrial targeting sequence of PB1-F2

To map the MTS of PB1-F2, we generated a panel of cDNAs encoding N- or C-terminal deletion mutants fused to 3xFLAG as a reporter on the N-terminal portion (Fig. 2) and analyzed the immunofluorescence distribution of each deletion mutant (Fig. 1). A series of N-terminally deleted mutants revealed that constructs expressing the PB1-F2 amino acids 12–87, 22–87, 31–87, 39–87, 46–87, 51–87, 61–87, 62–87 and 63–87 exhibited mitochondrial localization, whereas constructs expressing the PB1-F2 amino acids 64–87, 65–87 and 69–87 exhibited diffuse cytoplasmic fluorescence. These results indicated that the N-terminal border of the PB1-F2 MTS was between Ser63 and Leu64. On the other hand, a series of C-terminally deleted mutants showed that constructs expressing the PB1-F2 amino acids 1–87, 1–76 and 1–75 exhibited mitochondrial localization, whereas constructs expressing the PB1-F2 amino acids 1–74, 1–73, 1–72, 1–71 and 1–63 exhibited diffuse cytoplasmic fluorescence. These results indicated the C-terminal border of PB1-F2 MTS to be between Thr74 and Arg75. We further analyzed the PB1-F2 MTS domain that is necessary and sufficient for mitochondrial localization of its fusion protein. Constructs expressing PB1-F2 amino acids 22–75, 31–75 and 46–75 (Fig. 1J–L) fused to 3xFLAG in the N-terminal region localized in mitochondria, but 56–75 and 63–75 (Fig. 1M–O) had a cytoplasmic localization. These results suggest that the PB1-F2 residues in 46–75 are necessary and sufficient MTS. To confirm this finding, we expressed PB1-F2 amino acids 46–75, 56–75 and 63–75 fused to EGFP in the N-terminal region and further analyzed their localization in transfected cells. EGFP-PB1-F2-46/75 localized in mitochondria, but EGFP-PB1-F2-56/75 and -63/75 did not (Fig. 1P–R). From these results, we concluded that the PB1-F2 residues in 46–75 were necessary and sufficient for chimeric proteins fused to the targeting element, and the PB1-F2 residue strip 63–75 was a minimal requirement for mitochondrial localization. As positively charged residues are commonly used

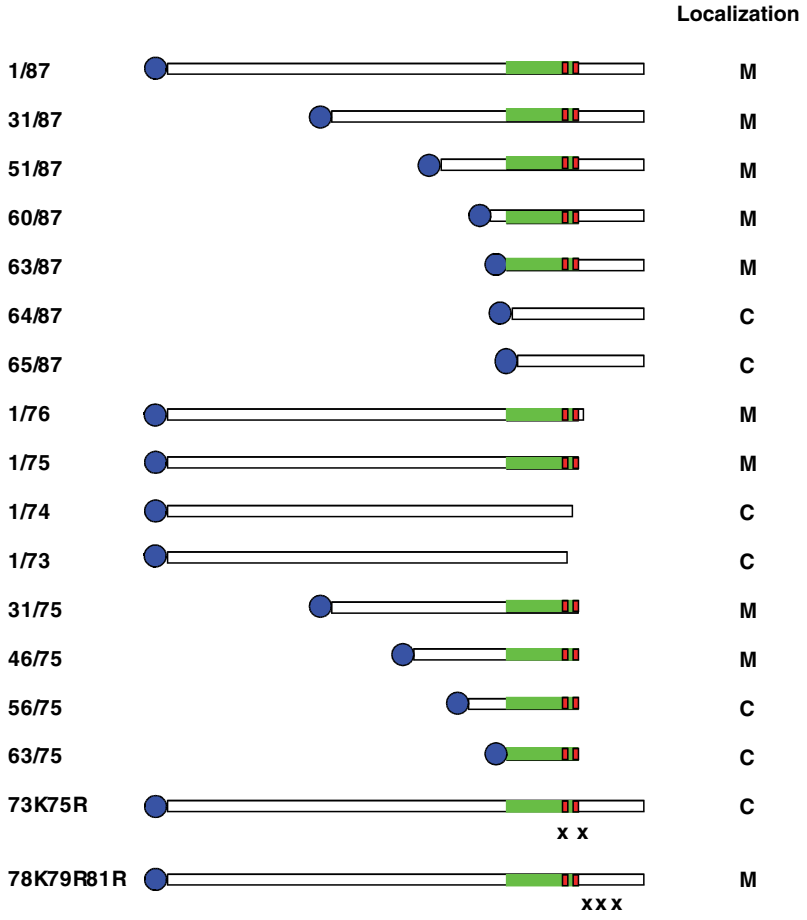

Fig. 2. A part of the chimeric 3xFLAG-PB1-F2 fusion constructs utilized in this study. The residues incorporated in the fusion proteins are shown on the left. Blue dots signify 3xFLAG. Green segments containing two red squares (basic residues K73 and R75) represent the minimal MTS of PB1-F2 (amino acids 63–75). All fusion proteins contain a linker residue (Leu) between 3xFLAG and the PB1-F2 sequence. "x" indicates the replaced basic residues. The intracellular localization of the fusion proteins is summarized on the right as follows: M, mitochondrial; C, cytoplasmic.

to target cellular proteins to mitochondria, we next examined the effect of a replacement of the basic residues with neutral residues in the predicted PB1-F2 MTS. Replacement of Lys and Arg residues in the C-terminal region at positions 73, 75, 78, 79 and 81 with Ala (K73A/R75A/K78A/R79A/R81A) completely abolished mitochondrial localization of 3xFLAG-PB1-F2, as reported previously [3]. However, replacement of Lys and Arg residues with Ala at positions 78, 79 and 81 (K78A/R79A/R81/A) did not change the localization (Fig. 1S–U). However, replacement of Lys and Arg residues with Ala at positions 73 and 75 in the predicted PB1-F2 MTS (K73A/R75A) completely abolished mitochondrial localization (Fig. 1V–X). These results revealed that the two positively charged residues at 73 and 75 in the predicted PB1-F2 MTS were minimally required for mitochondrial targeting, but the other positively charged residues in PB1-F2 were not essential.

3.3. Effects of PB1-F2 expression on mitochondrial morphology and function

It has been reported that the presence of PB1-F2 in the mitochondria of IAV-infected cells is associated with a loss of mitochondrial potential and mitochondrial rounding [2,3]. To confirm the functional similarity between the chimeric protein and PB1-F2, we analyzed the mitochondrial morphology and potential in cells expressing 3xFLAG-PB1-F2. As shown in Fig. 3A–C, 11 ± 1.2% of 3xFLAG-PB1-F2-expressing cells exhibited a change in the mitochondrial morphology with an isolated and vesicular pattern, compared with non-expressing cells with the normal interconnected and filamentous mitochondrial pattern. In contrast, expression of the fusion protein of *Discocoma* sp. red fluorescent protein and the mitochondrial targeting sequence from the subunit VIII of human cytochrome *c* oxidase did not modify mitochondrial morphology and typical filamentous mitochondria were observed (data not shown). The results suggested that the change in the mitochondrial morphology in 3xFLAG-PB1-F2 expressing cells was not an artifact of the overexpression of a mitochondrial protein.

We also analyzed suppression of mitochondrial membrane potential (MMP) of 3xFLAG-PB1-F2 expressing cells within mitochondria by a decreased accumulation of MMP-sensitive dye MitoTracker Red [22,23]. In the cells expressing 3xFLAG-PB1-F2 within mitochondria, 48 ± 2.8% of cells displayed a selective loss of mitochondrial MitoTracker Red staining (Fig. 3D–F). However, the cells transfected with 3xFLAG-PB1-F2 mutants which do not localize in mitochondria, such as 1/74 and 64/87, did not show a loss of MitoTracker Red staining (data not shown). We then analyzed the loss of MMP by using other MMP-sensitive probes, such as TMRE (Fig. 3G–I) and Rhodamine 123 (data not shown), and the results obtained confirmed the findings with MitoTracker Red staining. These results suggested that the 3xFLAG-PB1-F2 expression in mitochondria induces a loss of MMP, as reported for IAV-infected cells [2,3].

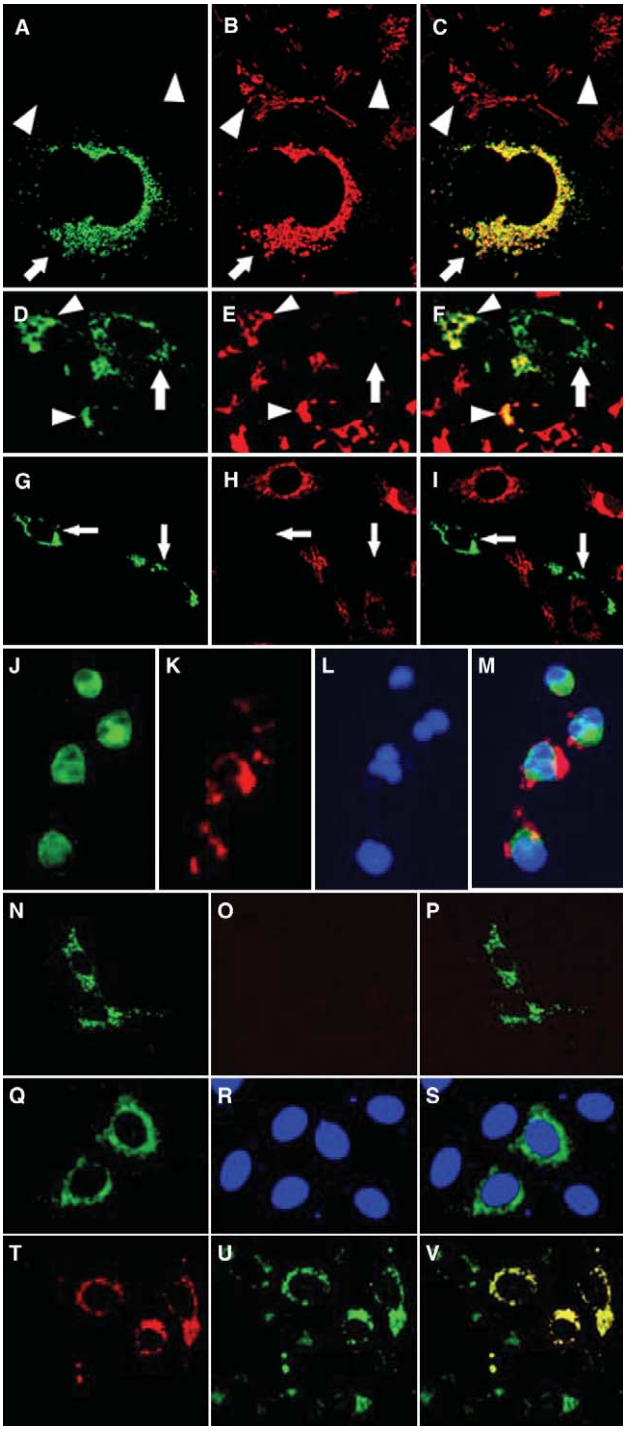

Fig. 3. Effects of PB1-F2 on transfected Vero cells. Vero cells transfected with a plasmid expressing 3xFLAG-PB1-F2 were incubated with MitoTracker Red (A–F) or with TMRE (G–I). Cells were fixed, permeabilized and analyzed by indirect immunofluorescence with mouse anti-FLAG monoclonal antibodies and FITC-conjugated anti-mouse antibodies. (A–C) Fluorescent signals were analyzed with a LSM 510 confocal microscope. An arrow and multiple arrowheads indicate the PB1-F2-expressing and not-expressing cells, respectively. (D-I) Multiple arrows and a single arrowhead indicate the PB1-F2-expressing cells with and without MitoTracker Red (D–F) or TMRE (G–I) staining, respectively. (J–M) Vero cells infected with influenza virus PR8 were incubated with annexin V conjugated with Alexa Fluor 594 (red) and fixed 24 h after infection. Cells were permeabilized and analyzed by indirect immunofluorescence with mouse anti-cytochrome *c* monoclonal antibodies and FITC-conjugated anti-mouse antibodies (green) and Hoechst 33342 staining (blue). (N–V) Vero cells transfected with plasmids expressing 3xFLAG-PB1-F2 were fixed 24 h after transfection. (N–P) 3xFLAG-PB1-F2 (green) and annexin V (red) were stained. (Q–S) 3xFLAG-PB1-F2 (green) and nuclear DNA (blue) were stained. (T–V) 3xFLAG-PB1-F2 (red) and cytochrome *c* (green) were stained.

In the mitochondria-mediated apoptotic process, the release of cytochrome *c* and apoptosis-inducing factors from mitochondria is accompanied by a loss of MMP and mitochondrial swelling [23]. We analyzed whether the mere targeting of PB1-F2 to mitochondria is a sufficient apoptotic trigger or not, in comparison with IAV-infected cells. As shown in Fig. 3J–M, almost all Vero cells infected with IAV exhibited the reported hallmarks of apoptosis [24], such as phosphatidylserine exposure on the outer leaflet of the plasma membrane detected by annexin V staining [25], nuclear condensation by Hoechst 33342 staining and release of cytochrome *c* from mitochondria into the cytosol. In these experiments, we confirmed IAV infection by using anti-influenza antibodies. In contrast to the IAV-infected cells, however, annexin V staining (Fig. 3N–P) and nuclear condensation (Fig. 3Q–S) were little detected in the 3xFLAG-PB1-F2-expressing cells. In addition, cytochrome *c* was predominantly detected in the mitochondria but not in the cytosol in the 3xFLAG-PB1-F2-expressing cells (Fig. 3T–V). Similar results were obtained in transfected HeLa and MDCK cells (data not shown). Taken together with these results, the targeting of 3xFLAG-PB1-F2 to mitochondria by itself might not be a sufficient factor for induction of apoptosis.

4. Discussion

Initiation of mitochondrial damages by IAV infection as well as apoptosis is a principal pathogenicity of IAV infection [2,11,12] and influenza associated encephalopathy [26]. We report here the MTS of the newly identified virus protein PB1-F2 and its function in mitochondria. Gibbs et al. [3] have shown that the amino acid residues of PB1-F2 69–82 are the minimal MTS by analyzing intracellular localization of the chimeric PB1-F2 protein fused to a relatively large molecular mass of 29 kDa EGFP at the C-terminus. In our follow-up experiments of the MTS, we found that efficiency of mitochondrial targeting of the chimeric PB1-F2-EGFP was low at $14 \pm 1.5\%$ in comparison with the efficiency of PB1-F2 at about 70% of PB1-F2-positive cells after infection of HeLa cells with influenza virus PR8. To bring the targeting efficiency of the chimeric PB1-F2 protein close to the native one, we made chimeric protein consisting of PB1-F2 fused to a small 2.9 kDa reporter protein 3xFLAG instead of EGFP and then analyzed the efficiency of mitochondrial targeting. In our assay conditions, we achieved mitochondrial localization of the 3xFLAG-PB1-F2 at $75 \pm 4\%$ in the PB1-F2-positive cells (Fig. 1D–F) being similar to the rate of native PB1-F2 (Fig. 1A–C). Analysis of the N- and C-terminal deletion mutants of PB1-F2 fused to a 3xFLAG at the N-terminus showed that the residues 46–75 were necessary and sufficient, and the residues 63–75 and both Lys73 and Arg75 were minimal requirements for mitochondrial localization (Figs. 1 and 2). Although the mapped minimal essential MTS determined by PB1-F2-EGFP as reported [3] and by 3xFLAG-PB1-F2 in our experiments were overlapped in the residues 69–75, the difference of the MTS between them might be due to the steric hindrance of chimeric PB1-F2 by the molecular size of reporter protein and/or the positions of tags at the N- or C-terminus for fusion. It has been well known that positively charged amphipathic helices are commonly used to target cellular proteins to mitochondria [27] and PB1-F2 has predicted α-helical regions between amino acids 54–62 and 73–82 [3]. These findings suggested that, in addition to the minimal essential MTS of the residues 63–75, α-helical region of the residues 54–62 may be important for sufficient mitochondrial localization of PB1-F2. The expression of PB1-F2 resulted in specific alterations in mitochondrial morphology and distribution (Fig. 3A–C). It is established that the mitochondria are highly dynamic organelles that are typically organized in the form of a continuous reticulum, but can be fragmented into smaller, tubular structures depending on the cell stage. The mitochondrion is fragmented during the S phase, but the organelle is organized as a reticulum in the G1 phase [28]. It has recently been shown that human T cell leukemia virus type 1 (HTLV-1) p13, the preceding viral protein that induces a morphological change of mitochondria into round-shaped clusters, suppresses tumor growth and cell proliferation [29,30]. Thus, it may be hypothesized that PB1-F2 affects the cell cycle and detains it at the S phase. Furthermore, about one half of the mitochondrial PB1-F2-expressing cells showed a decrease in the staining with MitoTracker Red (Fig. 3D–F), TMRE (Fig. 3G–I) and Rhodamine 123 (data not shown), suggesting a loss of MMP as a result of depolarization of the transmembrane potential. It has been reported that the opening of high conductance permeability transition pores in the mitochondrial inner membrane initiates the mitochondrial permeability transition and the loss of MMP, leading to mitochondrial depolarization, and an uncoupling of oxidative phosphorylation, which in turn leads to ATP depletion and apoptosis [31,32]. However, we could not detect any significant apoptotic signals by annexin V staining (Fig. 3N–P), Hoechst 33342 staining (Fig. 3Q–S), the release of cytochrome *c* from mitochondria (Fig. 3T–V) and DNA-laddering (data not shown) in PB1-F2-expressing Vero, HeLa and MDCK cells, although apparent apoptosis along with a loss of MMP in these cells was detected by infection of influenza virus. Gibbs et al. [3] have previously reported that the expression of PB1-F2-65/87-EGFP in transfected HeLa cells suppresses the MMP, but PB1-F2-1/87-EGFP does not, although the mechanisms of the difference in the effects between them have not been clarified. In addition to these findings, our data proposed a hypothesis that PB1-F2 expression alone is not sufficient for the initiation of apoptosis. In contrast, Chanturiya et al. [33] have recently shown that PB1-F2 creates variably sized pores in planar lipid membranes and may induce the permeabilization and destabilization of mitochondrial membranes. Further studies on the mechanisms of PB1-F2 in mitochondrial damage are now under investigation.

Acknowledgment: This study was supported in part by grants from the Cluster project and Grants-in-Aid (13557014 and 16790580) of Japanese Ministry of Education, Culture, Sports, Science and Technology. We appreciate review of the manuscript prior to submission by Pacific Edit.

References

[1] Kim, H.W., Brandt, C.D., Arrobio, J.O., Murphy, B., Chanock, R.M. and Parrott, R.H. (1979) Am. J. Epidemiol. 109, 464–479.
[2] Chen, W., Calvo, P.A., Malide, D., Gibbs, J., Schubert, U., Bacik, I., Basta, S., O'Neill, R., Schickli, J., Palese, P.,

Henklein, P., Bennink, J.R. and Yewdell, J.W. (1994) Nat. Med. 7, 1306–1312.
[3] Gibbs, J.S., Malide, D., Hornung, F., Bennink, J.R. and Yewdell, W. (2003) J. Virol. 77, 7214–7224.
[4] Aragon, T., de la Luna, S., Novoa, I., Carrasco, L., Ortin, J. and Nieto, A. (2000) Mol. Cell. Biol. 20, 6259–6268.
[5] Bui, M., Wills, E.G., Helenius, A. and Whittaker, G.R. (2000) J. Virol. 74, 1781–1786.
[6] de la Luna, S., Fortes, P., Beloso, A. and Ortin, J. (1995) J. Virol. 69, 2427–2433.
[7] Holsinger, L.J., Nichani, D., Pinto, L.H. and Lamb, R.A. (1994) J. Virol. 68, 1551–1563.
[8] Sakaguchi, A., Hirayama, E., Hiraki, A., Ishida, Y. and Kim, J. (2003) Virology 306, 244–253.
[9] Qian, X.Y., Alonso-Caplen, F. and Krug, R.M. (1994) J. Virol. 68, 2433–2441.
[10] O'Neill, R.E., Talon, J. and Palese, P. (1998) EMBO J. 17, 288–296.
[11] Woodfin, B.M. and Kazim, A.L. (1993) Arch. Biochem. Biophys. 306, 427–430.
[12] Mazo, E.L., Rusiaev, V.A., Fedorov, A.N., Iaroslavtseva, N.G. and Kharitonenkov, I.G. (1988) Vopr. Virusol. 33, 153–157.
[13] Takizawa, T., Matsukawa, S., Higuchi, Y., Nakamura, S., Nakanishi, Y. and Fukuda, R. (1993) J. Gen. Virol. 74, 2347–2355.
[14] Takizawa, T., Ohashi, K. and Nakanishi, Y. (1996) J. Virol. 70, 8128–8132.
[15] Fujimoto, I., Takizawa, T., Ohba, Y. and Nakanishi, Y. (1998) Cell Death Differ. 5, 426–431.
[16] Takizawa, T., Tatematsu, C., Ohashi, K. and Nakanishi, Y. (1999) Microbiol. Immunol. 43, 245–252.
[17] Schultz-Cherry, S. and Hinshaw, V.S. (1996) J. Virol. 70, 8624–8629.
[18] Ohyama, K., Nishina, M., Yuan, B., Bessho, T. and Yamakawa, T. (2003) Biol. Pharm. Bull. 26, 141–147.
[19] Schultz-Cherry, S., Dybdahl-Sissoko, N., Neumann, G., Kawaoka, Y. and Hinshaw, V.S. (2001) J. Virol. 75, 7875–7881.
[20] Zhirnov, O.P., Konakova, T.E., Wolff, T. and Klenk, H.D. (2002) J. Virol. 76, 1617–1625.
[21] Chen, H., Detmer, S.A., Ewald, A.J., Griffin, E.E., Fraser, S.E. and Chan, D.C. (2003) J. Cell Biol. 160, 189–200.
[22] Ishihara, N., Jofuku, A., Eura, Y. and Mihara, K. (2003) Biochem. Biophys. Res. Commun. 301, 891–898.
[23] Liu, X., Kim, C.N., Yang, J., Jemmerson, R. and Wang, X. (1996) Cell 86, 147–157.
[24] Kurokawa, M., Koyama, A.H., Yasuoka, S. and Adachi, A. (1999) Int. J. Mol. Med. 3, 527–530.
[25] Andree, H.A., Reutelingsperger, C.P., Hauptmann, R., Hemker, H.C., Hermens, W.T. and Willems, G.M. (1990) J. Biol. Chem. 265, 4923–4928.
[26] Yao, D., Chen, Y., Kuwajima, M., Shiota, M. and Kido, H. (2004) Biol. Chem. 385, 487–492.
[27] Endo, T. and Kohda, D. (2002) Biochim. Biophys. Acta 1592, 3–14.
[28] Capaldi, R.A. (2000) Trends Biochem. Sci. 25, 212–214.
[29] Ciminale, V., Zotti, L., D'Agostino, D.M., Ferro, T., Casareto, L., Franchini, G., Bernardi, P. and Chieco-Bianchi, L. (1999) Oncogene 18, 4505–4514.
[30] Silic-Benussi, M., Cavallari, I., Zorzan, T., Rossi, E., Hiraragi, H., Rosato, A., Horie, K., Saggioro, D., Lairmore, M.D., Willems, L., Chieco-Bianchi, L., D'Agostino, D.M. and Ciminale, V. (2004) Proc. Natl. Acad. Sci. USA 101, 6629–6634.
[31] De Vos, K., Goossens, V., Boone, E., Vercammen, D., Vancompernolle, K., Vandenabeele, P., Haegeman, G., Fiers, W. and Grooten, J. (1998) J. Biol. Chem. 273, 9673–9680.
[32] Petronilli, V., Nicolli, A., Costantini, P., Colonna, R. and Bernardi, P. (1994) Biochim. Biophys. Acta 1187, 255–259.
[33] Chanturiya, A.N., Basanez, G., Schubert, U., Henklein, P., Yewdell, J.W. and Zimmerberg, J. (2004) J. Virol. 78, 6304–6312.